UCLA
UCLA Previously Published Works

Title

Bone mineral density loss in thoracic and lumbar vertebrae following radiation for abdominal cancers

Permalink

https://escholarship.org/uc/item/44q0j258

Journal

Radiotherapy and Oncology, 118(3)

ISSN

0167-8140

Authors

Wei, Randy L
Jung, Brian C
Manzano, Wilfred
et al.

Publication Date

2016-03-01

DOI

10.1016/j.radonc.2016.03.002

Peer reviewed

eScholarship.org Powered by the California Digital Library
University of California

Radiotherapy and Oncology 118 (2016) 430–436

Contents lists available at ScienceDirect

Radiotherapy and Oncology

journal homepage: www.thegreenjournal.com

Vertebral metastatic fractures

Bone mineral density loss in thoracic and lumbar vertebrae following radiation for abdominal cancers

Randy L. Wei [a,1], Brian C. Jung [a,1], Wilfred Manzano [a], Varun Sehgal [a], Samuel J. Klempner [b], Steve P. Lee [c], Nilam S. Ramsinghani [a], Chandana Lall [d,*]

[a] Department of Radiation Oncology; [b] Department of Medicine, Division of Hematology-Oncology, University of California Irvine, Orange; [c] Department of Radiation Oncology, David Geffen School of Medicine, University of California Los Angeles; and [d] Department of Radiology, University of California Irvine, Orange, USA

ARTICLE INFO

Article history:
Received 28 September 2015
Received in revised form 1 March 2016
Accepted 1 March 2016
Available online 15 March 2016

ABSTRACT

Purpose: To investigate the relationship between abdominal chemoradiation (CRT) for locally advanced cancers and bone mineral density (BMD) reduction in the vertebral spine.

Materials and methods: Data from 272 patients who underwent abdominal radiation therapy from January 1997 to May 2015 were retrospectively reviewed. Forty-two patients received computed tomography (CT) scans of the abdomen prior to initiation and at least twice after radiation therapy. Bone attenuation (in Hounsfield unit) (HU) measurements were collected for each vertebral level from T7 to L5 using sagittal CT images. Radiation point dose was obtained at each mid-vertebral body from the radiation treatment plan. Percent change in bone attenuation (Δ%HU) between baseline and post-radiation therapy were computed for each vertebral body. The Δ%HU was compared against radiation dose using Pearson's linear correlation.

Results: Abdominal radiotherapy caused significant reduction in vertebral BMD as measured by HU. Patients who received only chemotherapy did not show changes in their BMD in this study. The Δ%HU was significantly correlated with the radiation point dose to the vertebral body ($R = -0.472$, $P < 0.001$) within 4–8 months following RT. The same relationship persisted in subsequent follow up scans 9 months following RT ($R = -0.578$, $P < 0.001$). Based on the result of linear regression, 5 Gy, 15 Gy, 25 Gy, 35 Gy, and 45 Gy caused 21.7%, 31.1%, 40.5%, 49.9%, and 59.3% decrease in HU following RT, respectively. Our generalized linear model showed that pre-RT HU had a positive effect ($\beta = 0.830$) on determining post-RT HU, while number of months post RT ($\beta = -0.213$) and radiation point dose ($\beta = -1.475$) had a negative effect. A comparison of the predicted versus actual HU showed significant correlation ($R = 0.883$, $P < 0.001$) with the slope of the best linear fit = 0.81. Our model's predicted HU were within ±20 HU of the actual value in 53% of cases, 70% of the predictions were within ±30 HU, 81% were within ±40 HU, and 90% were within ±50 HU of the actual post-RT HU. Four of 42 patients were found to have vertebral body compression fractures in the field of radiation.

Conclusions: Patients who receive abdominal chemoradiation develop significant BMD loss in the thoracic and lumbar vertebrae. Treatment-related BMD loss may contribute to the development of vertebral compression fractures. A predictive model for post-CRT BMD changes may inform bone protective strategies in patients planned for abdominal CRT.

© 2016 Elsevier Ireland Ltd. All rights reserved. Radiotherapy and Oncology 118 (2016) 430–436

Vertebral body insufficiency and compression fractures are most commonly caused by osteoporosis, an age-related and systemic skeletal disorder characterized by compromised bone strength and low bone mineral density [1]. Although, most fractures are asymptomatic, the degree of BMD loss, location of the fracture, and secondary osteoporosis from underlying medical condition including chemotherapy may make an asymptomatic, stable fracture more prone to progressive collapse causing pain, loss of mobility, and spinal cord compression [2]. The overall morbidity of vertebral body compression fractures is significant, and women diagnosed with compression fractures have a 15% higher mortality rate than matched controls [3].

Irradiation of normal, non-malignant bone results in small vessel damage leading to microcirculatory occlusion, marrow hypocellularity from death of osteoblast and osteoclast, and fatty

* Corresponding author at: University of California Irvine, Department of Radiology, 101 The City Drive South, Orange, CA 92868, USA.
E-mail address: clall@uci.edu (C. Lall).
[1] These authors contributed equally to this work.

http://dx.doi.org/10.1016/j.radonc.2016.03.002
0167-8140/© 2016 Elsevier Ireland Ltd. All rights reserved.

marrow replacement [4–7]. Several reports have shown BMD reduction after radiation to the pelvis, cervical vertebrae, and thoracic rib [8,9]. Advances in 3D Conformal Radiation Therapy, Intensity Modulated Radiation Therapy (IMRT), and Volumetric Modulated Arc Therapy (VMAT) have improved dose delivery accuracy, increased dose to target, reduced treatment time, and avoided integral dose of radiation to organs at risk (OAR) including lungs, heart, kidneys, and spinal cord. However, improved dose conformity to the target using IMRT/VMAT can potentially lead to an increased dose to anatomical structures outside of the planning treatment volume including to the nearby vertebral bodies.

Although dual-energy X-ray absorptiometry (DEXA) serves as the gold standard for BMD quantification, several studies have determined that the BMD provided by DEXA has a strong correlation with CT-derived Hounsfield units (HU), can provide reliable estimates for regional bone strength and BMD, and accurately rule out osteoporosis with better than 90% sensitivity [10–13]. Since diagnostic CT scans are ordered routinely to monitor response to treatments, we can utilize CT-derived HU to monitor BMD in patients, while avoiding the need for additional DEXA imaging and improving resource utilization.

The purpose of the study was to investigate whether patients undergoing abdominal radiation would develop radiation-induced thoracic and lumbar vertebrae BMD loss. We developed a model to accurately predict the degree of change in a patient vertebral BMD based on bone attenuation prior to abdominal radiation therapy, radiation dose to the vertebral body, and the elapsed time from radiation.

Materials and methods

Patients

A retrospective search of our institution's database identified 272 patients who underwent radiation therapy for a tumor of the abdominal origin (pancreatic, esophageal, gastric, and hepatobiliary) from January 1997 to January 2015. This study was approved by the institutional review board (HS# 2015-2048). Patients who had a baseline CT scan prior to radiation therapy, and at least two CT scans beginning three months post radiation therapy ($N = 42$) were included. Pre-specified patient stratification included months between the completion of radiation therapy and the date of their CT imaging (group 1: 4–8 months; group 2: >9 months). CT scans were ordered at the discretion of the patient's oncologist.

Post-hoc analyses further examined patients who had a CT scan greater than 5 months post-radiation therapy ($N = 32$). Patients with abdominal cancers who received chemotherapy, but did not receive radiation therapy served as controls ($N = 6$). Patients with spinal instrumentations and metastatic disease to the spine were excluded.

Imaging

Computed tomography

Multi-slice CT imaging was performed on Philips platform iCT 256 channel scanners (Philips Healthcare, Andover, MA). Volumetric data acquisition was obtained with 3 mm axial, coronal, and sagittal image reconstructions. Dose modulation was used routinely in all CT scanners on every slice depending on patient's body habitus. IMPAX volume viewing software (AGFA HealthCare Corporation, Greenville, SC) was used to calculate the mean bone attenuation of each vertebra on sagittal view. Mean bone attenuation of T7 to L5 vertebrae were measured using HU. A circular region of interest (ROI) with an area ranging from 100 to 120 mm^2 was placed manually on the cancellous bone area avoiding subchondral sclerotic bone and pre-existing fractures. The size of the ROI was kept constant throughout all vertebral levels (Supplemental Fig. 1). Detailed methods for ROI delineation and calculating HU can be found in the supplementary information. Two independent raters blinded to radiation dose data determined pre-radiation therapy HU (HU_{pre}) and post-radiation therapy (HU_{post}) data.

Eclipse Radiation treatment planning software (Varian, Palo Alto, CA) was used for generating the patient treatment plans. The radiation point dose was calculated at each vertebral level extending from T7 to L5. The vertebral levels were determined on the sagittal view. Each vertebral body was divided into three vertical segments and the point dose was calculated at the middle of the vertebral body on axial slice at each vertical segment, yielding three values of point dose per vertebrae. These three point doses were then averaged to determine the final radiation dose in Gy for each vertebral body T7–L5.

Statistical analyses

Inter-rater reliability for the measurements of bone attenuation was assessed using intra-class correlation coefficient. Due to the difference in the HU across vertebral levels and across different patients at the time before the start of radiation therapy, percent decrease in bone attenuation (Δ%HU) for each vertebral level was calculated with the following equation (Eq. (1)):

$$\Delta\%\mathrm{HU} = \frac{\mathrm{HU_{post}} - \mathrm{HU_{pre}}}{\mathrm{HU_{pre}}} \tag{1}$$

To directly assess the effect of radiation dose on the change in Δ%HU, Pearson's correlation analysis was performed on Δ%HU and radiation dose. All vertebrae were divided based on the amount of radiation dose they received (<5 Gy; 5–15 Gy; 15–25 Gy; 25–35 Gy; and >35 Gy). For each group, the difference in Δ%HU as compared to the baseline was tested using the 2-tailed Student's *t*-test. The Bonferroni–Holm method was used to correct for the effects of multiple comparison. To ensure that there was no systematic bias associated with calculating HU on the sagittal axis images only, CT-attenuation from sagittal slices were compared to axial slices using Pearson's correlation analysis (see Supplementary information).

Predictive radiological factors that may modulate vertebral bone density were collected (α). Predictive factors (α) include: (1) HU_{pre}; (2) number of months between CT and the completion of radiation therapy (time); and (3) radiation dose to mid-vertebral body. The radiation dose was converted to biologically effective dose (BED_Gy_3) based on the following equation:

$$\mathrm{BED\_Gy_3} = \mathrm{nd}\left[1 + \frac{d}{3}\right]$$

where n is the number of fractions and d is the dose per fraction.

Patient's nutritional status prior to the start of their radiation therapy was then added as part of post hoc analyses. These factors included: (1) serum calcium level ($Calcium_{pre}$); (2) total protein level ($Protein_{pre}$); (3) total albumin level ($Albumin_{pre}$); and (4) patient's weight in kilogram before the start of their radiation therapy. The relative weighting of each of the predictive factors (δ) was calculated by multiplying the Moore–Penrose inverse of predictive factors (α) by the matrix of HU_{post} (β) as follows (Eq. (2)).

$$\left(\begin{bmatrix} \alpha_{1,1} & \cdots & \alpha_{1,m} \\ \vdots & \ddots & \vdots \\ \alpha_{n,1} & \cdots & \alpha_{n,m} \end{bmatrix}\right)^{+} * \begin{bmatrix} \beta_1 \\ \vdots \\ \beta_n \end{bmatrix} = \begin{bmatrix} \delta_1 \\ \vdots \\ \delta_m \end{bmatrix} \tag{2}$$

2.4 Model validation

The predictive model was validated using the Jackknife resampling method (see Supplementary information). Additionally, to investigate which clinical and radiological factors yielded the highest predictive power in predicting the post-radiation HU, we repeated Jackknife resampling with every combination of predictive factors. The number of correct predictions at the different allowed HU error thresholds was calculated for each combination of predictive factors and plotted against the allowed HU error threshold. Numerical integration using trapezoidal method (*trapz.m*, Matlab R2011b) was used to compute the area under the curve (AUC). The combination of factors with the highest AUC was determined to have the best predictive power.

3. Results

3.1 Patient characteristics

We identified 272 patients who underwent radiation for cancers of the abdomen. Of those, 42 patients had CT scan prior to chemo-radiation and two follow-up CT scans post radiation therapy. The mean age was 59.7 yrs (range, 42–78 years). There were 27 males and 15 females in the study population. The bile duct was the most common site of cancer (48%). Majority of the patients received concurrent chemotherapy with radiation. Patient's baseline calcium, protein, and albumin values were within normal limits. Patient demographics, labs values, radiation treatment, and chemotherapy are summarized in Table 1.

Table 1
Description of the study population ($n = 42$). 3D-CRT (Three Dimensional Conformal Radiotherapy), VMAT (Volumetric Modulated Arc Therapy).

Characteristic	N
Demographic	
Mean age (yrs)	59.7 (42–78)
Sex (Male / Female)	27/15
Location of cancer	
Stomach	9
Esophagus	4
Pancreas	9
Gallbladder	20
Laboratory values	
Mean calcium	9 (7.7–10.2)
Mean total protein	6.6 (4.1–7.8)
Mean albumin	3.5 (1.9–4.5)
Mean weight (kg)	75.5 (46.1–115.3)
Treatment plan	
Mean prescribed dose (Gy)	49.6 (37.5–52.5)
32.4 Gy / 1.8 Gy per fx	1
37.5 Gy / 2.5 Gy per fx	1
40.0 Gy / 2 Gy per fx	1
45.0 Gy / 1.8 Gy per fx	1
50.4 Gy / 1.8 Gy per fx	37
52.5 Gy / 2.1 Gy per fx	1
Radiation treatment delivery	
2 Field 3D-CRT	2
3 Field 3D-CRT	1
4 Field 3D-CRT	12
1 Arc VMAT	3
2 Arc VMAT	21
3 Arc VMAT	2
4 Arc VMAT	1
Chemotherapy before radiation therapy	
Gemcitabine	11
Gemcitabine + cisplatin	3
Gemictabine + capecitabine	3
Gemicitabine + erlotinib	6
Gemictabine + nab-paclitaxel	1
Capecitabine	2
Carboplatin	1
Carboplatin + taxol	2
Carboplatin + taxol + trastuzumab	2
FOLFOX	2
FOLFIRINOX	3
None	6
Chemotherapy after radiation therapy	
Capecitabine	32
Carboplatin + taxol	3
Carboplatin + taxol + trastuzumab	2
None	5

3.2 Abdominal CRT leads to BMD reduction

To determine if radiation can cause BMD reduction in the vertebrae, we measured the bone attenuation of each vertebrae body from pre-treatment CT and two subsequent post-treatment surveillance CT scans (Table 2). A representative patient's CT scan and measurements at baseline, 5 months and 12 months is seen in Fig. 1A-C. All attenuation measurements on CT showed excellent inter-observer reliability. Agreement was good across blinded radiologists with mean intra-class coefficient for inter-rater reliability of 0.901 (range: 0.832–0.942; $P < 0.001$) for bone attenuation. Direct comparison of bone attenuation collected from sagittal slices against bone attenuation collected from axial scans showed a strong linear correlation ($R = 0.994$, $P < 0.001$).

When the bone attenuation was plotted against the vertebral level, there was an acute reduction in bone attenuation in vertebral bodies that received radiation, whereas the vertebral bodies that received no radiation did not see a reduction in BMD (Fig. 1D). Fourteen patients had CT scan greater than 12 months after their radiation therapy. BMD reduction persisted after 12 months. A separate cohort of patients who received only chemotherapy did not show any change in bone attenuation ($p = 0.12$) (Fig. 1E).

To determine dose–response relationship between radiation dose and BMD reduction, we plotted each vertebrae's radiation dose to its respective Δ%HU. The correlation between the radiation dose and Δ%HU were evaluated using both factors as continuous variables. Within 4–8 months after completion of radiation, vertebrae that had received radiation had a significant reduction ($R = -0.472$, $P < 0.001$) in BMD (Fig. 2A). The dose–response relationship persisted in subsequent scans after 9 months ($R = 0.578$, $P < 0.001$) (Fig. 2B).

In post hoc analysis, only patients who had a CT scan greater than 5 months post-radiation therapy were included for further analyses ($N = 32$). The average time between the end of radiation therapy and their follow-up CT scan was 9.2 months. Consistent with the prior analysis, the percent change in bone attenuation following radiation therapy significantly correlated with radiation dose ($R = 0.578$, $P < 0.001$). Based on the results of linear regression analysis, 5 Gy, 15 Gy, 25 Gy, 35 Gy, and 45 Gy dose on the vertebrae caused 21.7%, 31.1%, 40.5%, 49.9%, and 59.3% decrease in HU after radiation therapy, respectively. The relationship between radiation dose and the percent change in bone attenuation following radiation therapy did not differ between thoracic and lumbar spine ($P > 0.17$).

Table 2
Relationship between radiation dose deposited to vertebral body and change in HU at two interval time periods following radiation.

Vertebral Body Radiation Dose	4–8 months		9–12 months	
	Avg $\Delta\%HU_{post}$	*P* Value	Avg $\Delta\%HU_{post}$	*P* Value
<5 Gy	13.7 ± 18.8%	0.021	19.2 ± 18.4%	<0.001
5–15 Gy	27.9 ± 22.9%	0.103	33.9 ± 20.0%	<0.001
15–25 Gy	37.5 ± 17.5%	<0.001	47.1 ± 23.4%	<0.001
25–35 Gy	43.3 ± 25.7%	<0.001	52.1 ± 19.8%	<0.001
>35 Gy	40.2 ± 33.5%	<0.001	51.7 ± 25.4%	0.001

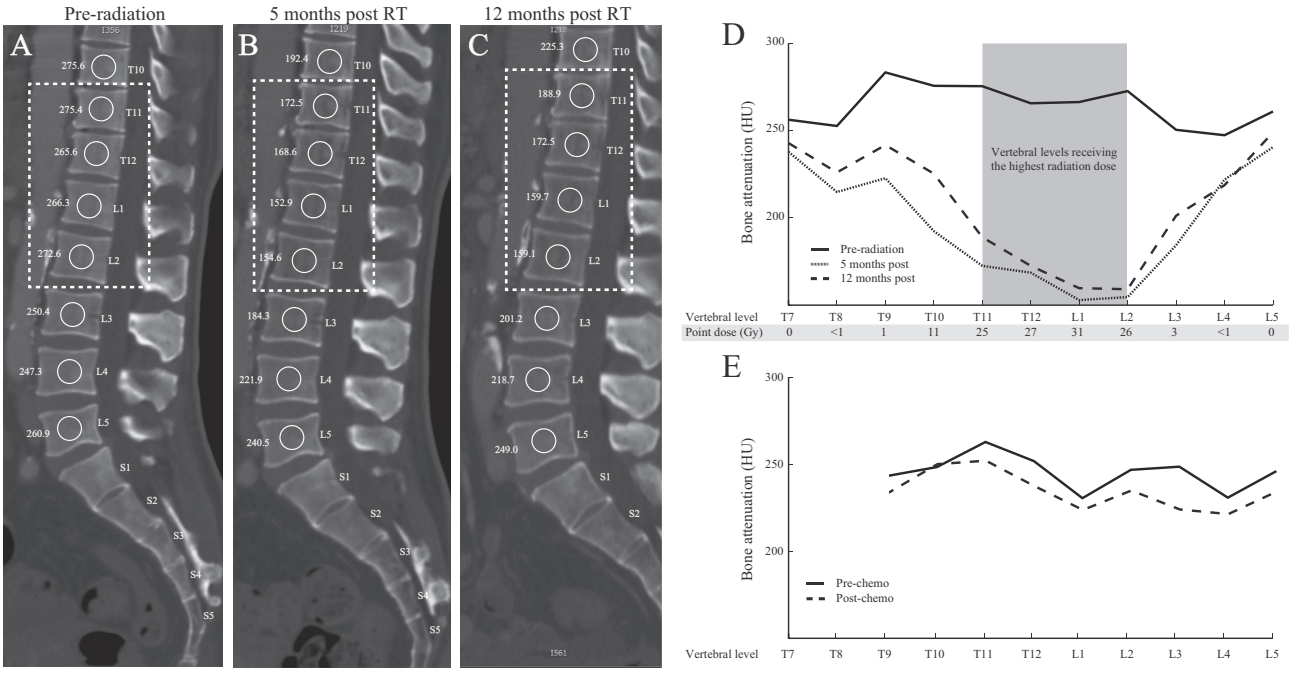

Fig. 1. Sagittal view of patient prior to radiation (A), 5 months after radiation therapy (B), and 12 months after therapy (C). Dashed white box encompasses the vertebrates that received the highest radiation doses. (D) Bone attenuation was plotted to respective vertebral level and its radiation dose. Gray zone highlights T11–L2, which had the greatest bone attenuation change and the highest radiation doses. (E) There was no change in bone attenuation in patients who received chemotherapy alone.

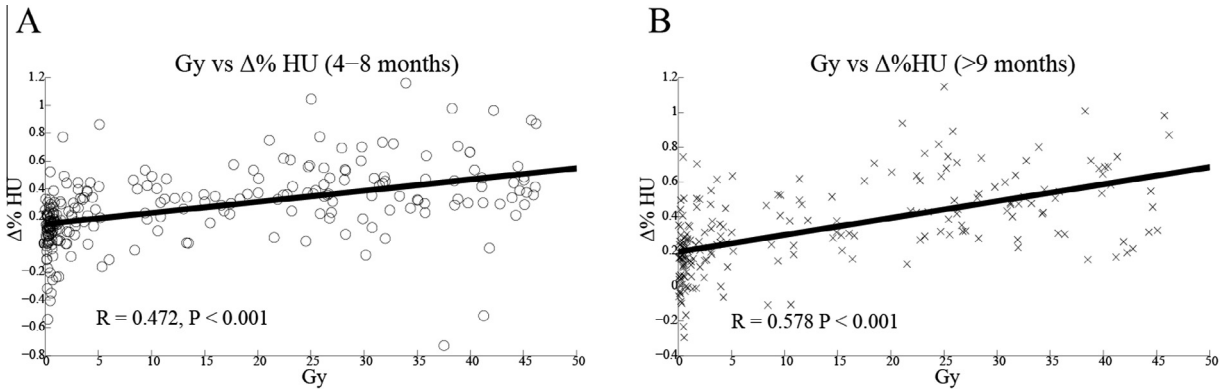

Fig. 2. Individual vertebral body Δ%HU correlates with received dose at two different interval periods following radiation. Patients are sub-divided into three groups based on the number of months between the date of their CT scan and the end date of their radiation therapy (group 1: 4–8 months (A); group 2:>9 months (B). For both groups, Δ%HU significantly correlated with Gy ($R > 0.472$, $P < 0.001$). Black line demonstrates the best linear fit.

To determine the consequence of BMD reduction, a radiologist reviewed the CT scans of all patients for compression fractures after completion of radiation therapy (Fig. 3). Two male patients with a new L2 vertebral compression fractures and one female patient with a new T12 vertebral compression fracture were identified on surveillance CT scan 38, 241, and 286 days after radiation therapy, respectively. To determine if vertebral compression fractures are seen after a year, we reviewed all followup CT scans for all the patients. We identified a fourth male patient with a new T11 vertebral compression fracture 449 days after radiation, and a fifth male with a new T11 and T12 vertebral compression fracture on a surveillance scan 1,008 days after completion of radiation therapy. All vertebral fractures were within the field of radiation. The CT scans that detected the vertebral compression fracture were requested for surveillance of their cancer and not for indication of back pain. None of the patients had evidence of metastatic disease at the time of the discovery of the vertebral fractures. The clinical information for the patients with vertebral compression fractures is shown in Supplemental Table 1.

3.3 Generalized linear model can predict the post-radiation bone attenuation

Given that BMD has a strong dose–response to radiation, we developed a generalized linear model to help predict the expected value of bone attenuation in a given vertebrae. Using bone attenuation measured prior to radiation, the biologically effective dose (BED_Gy_3) calculated from the total radiation dose to the vertebrae, and the number of months after radiation, we are able to predict the bone attenuation after radiation therapy. Our model predicted that an increase in HU_{pre} increases HU_{post} ($\beta = 0.830$). In contrast, an increase in $Months_{post}$ and BED_Gy_3 decreases HU_{post} (β = -0.213 and -1.475, respectively). Based on these findings, HU_{post} could be computed based on Eq. (3):

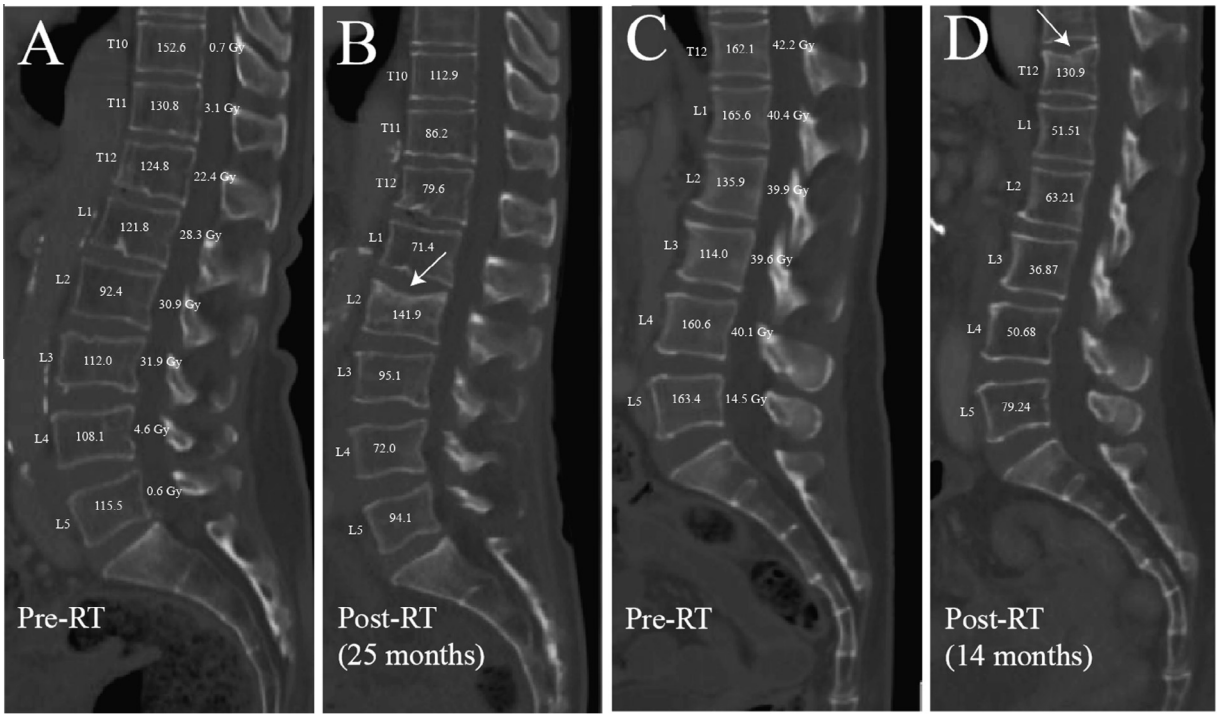

Fig. 3. Representative CT images of patient 1 and patient 2 (patient 1: A–B; patient 2: C–D) showing compression fracture before and after radiation therapy. Twenty-five months after the completion of radiation therapy, patient 1 showed a wedge compression in L2 (B), where the radiation dose was the highest (30.9 Gy). Patient 2 showed wedge compression in T12 at 14 months post-radiation therapy after receiving 42.2 Gy radiation dose to the vertebral body (D).

$$HU_{post} = (0.830 * HU_{pre}) + (-0.213 * \text{number of months post therapy}) + (-1.475 * BED\_Gy_3) \quad (3)$$

Comparison of the predicted HU_{post} versus the actual HU_{post} showed a significant linear correlation ($R = 0.883$, $P < 0.001$) with the slope of the best linear fit = 0.81 (Fig. 4A). Our model's predicted HU_{post} was within ±20 HU of the actual value in 53% of cases, 70% of the predictions were within ±30 HU, 81% of the predictions were within ± 40 HU, and 90% of the predictions were within ±50 HU of the actual HU_{post} (Fig. 4E).

3.4 Nutritional factors do not improve model performance

To determine whether nutritional status at the time of radiation treatment could improve the predictive power of our multiple linear regression model, we included differences in calcium, total protein, albumin, and the patient's weight in kilograms prior to the start of radiation therapy to test for a linear trend in relation to bone attenuation and radiation dose. All nutritional status factors ($Calcium_{pre}$, $Protein_{pre}$, $Albumin_{pre}$, $Weight_{pre}$) were included into the predictive factor matrix (α) with the predictive factors obtained from the radiological images. While the predictive power of the generalized linear model did improve with addition of each nutritional status variable, the difference was negligible (Fig. 4).

4. Discussion

Using retrospective data from a cohort of patients undergoing abdominal CRT we demonstrated that CRT results in vertebral BMD reduction in the field of radiation. There is a dose–response relationship between radiation delivered to vertebral body and BMD reduction, which can be predicted using RT and imaging characteristics. BMD changes can occur as early as four months from time of radiation and persist up to a year.

Our results demonstrate a proportional relationship between the radiation dose and degree of BMD reduction. Vertebral bodies receiving as little as 5 Gy had significant and persistent BMD reduction and insufficiency fractures. There is no commonly accepted dose tolerance for BMD reduction. Thus, radiation induced BMD reduction is likely a non-stochastic effect that does not have a dose threshold. In the pelvis, doses as low as 22.5 Gy resulted in BMD reduction *[14]*. The incidence of pelvic insufficiency fracture has been reported to increase if external radiation to the pelvic exceeds 45 Gy [4]. Clinicians need to be aware of this association and have a low clinical suspicion for vertebral compression fractures in post-CRT patients describing back pain, pain worse in standing position, pain alleviated in supine position, and limited spinal mobility. Additionally, follow up BMD monitoring, perhaps via CT scans should include assessment of insufficiency fractures that may be amenable to interventional treatments to strengthen the vertebrae body. Patients should undergo physical therapy to avoid falls, and counseled on avoiding strenuous lifting and bending. Lastly, patients may benefit from pharmacological management including bisphosphonates and denosumab therapy.

The mechanism underlying CRT-induced BMD changes is likely related to small vessel and capillary damage resulting in osteoclast and osteoblast cell death and resultant fatty infiltration of a hypocellular bone marrow [15]. The thoracic and lumbar vertebra are supported by a highly complex arterial plexus comprised of primary and secondary periosteal arterioles that interdigitate with adjacent vertebral body arterioles to form metaphyseal anastomoses between adjacent vertebral bodies [16]. Radiation may obliterate or cause inflammatory reaction causing occlusion of these micro-arterioles. Additionally, an older spine is more susceptible to disruptions in circulation from foraminal narrowing and increased coiling of central vertebral arteries ultimately increasing

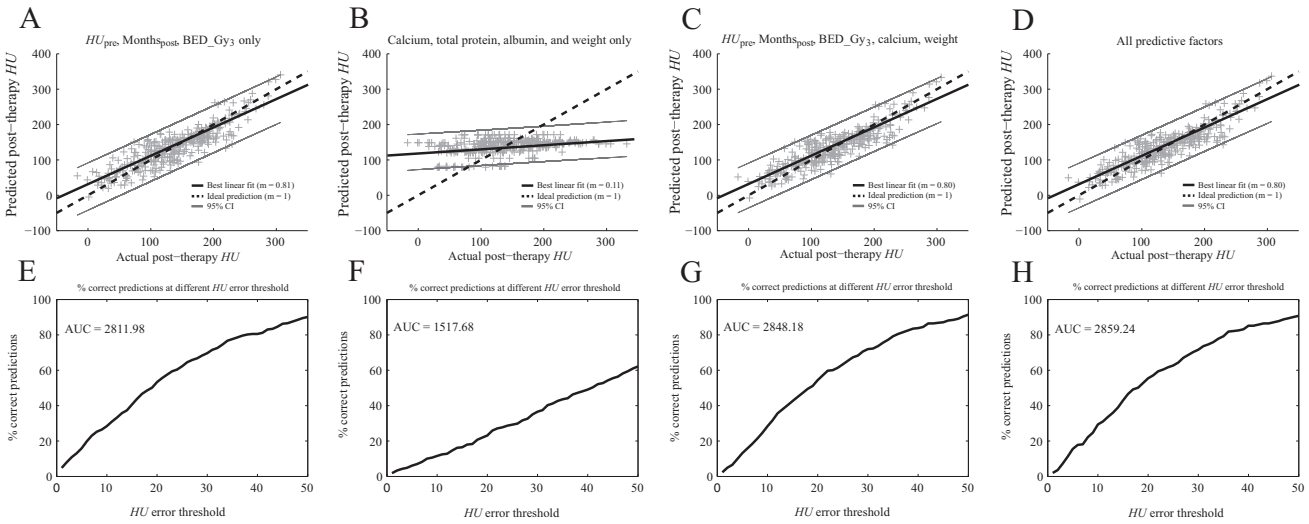

Fig. 4. Generalized linear model can predict the change in bone attenuation after radiation therapy. The patients' actual bone attenuation after radiation therapy was plotted against the bone attenuation that was predicted by our generalized linear model (A). Our predicted bone attenuation correlation with the actual HU_{post} ($R = 0.883$, $P < 0.001$). Different generalized linear models were created based on different combination of patients' nutritional status and radiological predictive factors (B–D). The% correct predictions at different bone attenuation error threshold was plotted and the area under the curve (AUC) was used as a surrogate marker for the predictive power of the generalized linear model (E–H). (B and F) Generalized linear model created using only the nutritional status factors showed poor predictive power (AUC = 1518.9). As compared to using only the radiological findings (AUC = 2812.0), including nutritional status in addition (C, D, G, H) did increase the predictive power of the generalized linear model, but the improvement was modest ($2848.2 \leqslant AUC \leqslant 2859.8$).

intraosseous ischemic conditions [17]. Our study supports the concept of taking planning measures to limit RT dose to vertebral bodies, especially in patients with pre-existing low HU reflecting underlying osteoporosis. Developing a model based on the metrics derived from CT HU and radiation dose received has immediate clinical utility. Our model was able to predict within ±30 HU with 70% accuracy. For example, patients predicted to have HU_{post} in the osteopenic and/or osteoporotic range (HU 100.8, 78.5 respectively) may warrant more aggressive monitoring and early medical therapy to minimize morbidity associated with fracture events. Similarly, particular attention to RT planning measures to reduce vertebral dose is important in low HU_{post} predictions. Beyond the scope of the current study, the variables of our generalized linear model could also be rearranged to compute the maximum radiation dose that is safe to deliver without increasing the risk of developing moderate BMD reduction.

There are several limitations to this study. First, we used CT-derived HU to estimate the degree of BMD reduction. Although the gold standard for measuring BMD is the DEXA scan, several studies demonstrate the utility of diagnostic CT scan in providing reliable estimates for regional bone strength and BMD [10–13]. Secondly, this study is a retrospective review of patients treated at a single institution. The results from this study will need to be validated in a larger, multi-institutional prospective trial. Although, DEXA scans would be the ideal method for monitoring BMD in a future study, DEXA scans are not a part of post-treatment care in patients with abdominal cancers. Thirdly, it is possible that the vertebral bodies with high HU prior to radiation therapy may respond differently to radiation as compared to the vertebral bodies with low baseline HU. We were statistically underpowered to generate a separate generalized linear model after reclassifying patients based on their baseline HU. Furthermore, it is possible that the factors used to compute the predictive model may have a non-linear correlation with the change in HU after radiation therapy. Presumably, the change in HU will be maximum immediately preceding radiation therapy and will stabilize over time to reach an asymptote; future studies must be conducted to investigate this relationship further. Fourthly, we calculated the radiation dose for each vertebra by averaging the point dose at three vertical segments of each vertebral body rather than calculating the mean dose of the entire vertebra using 3D planning. While the use of 3D planning could provide us with a more accurate representation of the radiation-associated changes in BMD, we chose to use the point dose method because we wanted to create a model with direct clinical applicability that is easy to use and readily accessible by all health care providers. Furthermore, point dose has been demonstrated to be a good predictor for risk of mandibular fracture [18]. Fifthly, most of our patients were treated by 50.4 Gy at 1.8 Gy per fraction. By converting the point dose to biologically effective dose, our generalized linear model would also be true for other dose-fractionation regimens; however, this must be validated prospectively. Lastly, to collect HU measurements from T7-L5 vertebrae, CT scans of the thorax and abdomen collected on same visit were used. Not all CT scans were acquired using the same acquisition sequence. Additionally, a few CTs were acquired from outside hospitals, which may be a confounding factor that could negatively affect the predictive power of our generalized linear model. Moreover, patients received chemotherapy as part of their treatment, and the effect of chemotherapy in addition to radiation on BMD is unknown. However, our control patients who received chemotherapy alone did not develop any BMD changes and no insufficiency fractures.

In conclusion, standard fractionation radiation for abdominal cancers results in BMD reduction of vertebrae bodies encompassed by the radiation treatment field. Our predictive model, based on CT-derived metrics, was able to predict the magnitude of the change in BMD reduction after radiation therapy. Predicting BMD helps to identify patients who may benefit from closer surveillance and early drug therapy initiation to prevent insufficiency fractures and vertebral compression, and may warrant dose reduction to the vertebral column to avoid further BMD reduction.

Conflict of interest statement

None of the authors have any conflict of interests.

Appendix A. Supplementary data

Supplementary data associated with this article can be found, in the online version, at http://dx.doi.org/10.1016/j.radonc.2016.03.002.

References

[1] Riggs BL et al. Differential changes in bone mineral density of the appendicular and axial skeleton with aging: relationship to spinal osteoporosis. J Clin Invest 1981;67:328–35.
[2] Lindsay R et al. Risk of new vertebral fracture in the year following a fracture. JAMA 2001;285:320–3.
[3] Cooper C et al. Population-based study of survival after osteoporotic fractures. Am J Epidemiol 1993;137:1001–5.
[4] Fu AL, Greven KM, Maruyama Y. Radiation osteitis and insufficiency fractures after pelvic irradiation for gynecologic malignancies. Am J Clin Oncol 1994;17:248–54.
[5] Hopewell JW. Radiation-therapy effects on bone density. Med Pediatr Oncol 2003;41:208–11.
[6] Mumber MP, Greven KM, Haygood TM. Pelvic insufficiency fractures associated with radiation atrophy: clinical recognition and diagnostic evaluation. Skeletal Radiol 1997;26:94–9.
[7] Sykes MP, Chu FC, Wilkerson WG. Local bone-marrow changes secondary to therapeutic irradiation. Radiology 1960;75:919–24.
[8] Huh SJ et al. Pelvic insufficiency fracture after pelvic irradiation in uterine cervix cancer. Gynecol Oncol 2002;86:264–8.
[9] Oh D et al. Pelvic insufficiency fracture after pelvic radiotherapy for cervical cancer: analysis of risk factors. Int J Radiat Oncol Biol Phys 2008;70:1183–8.
[10] Schreiber JJ et al. Hounsfield units for assessing bone mineral density and strength: a tool for osteoporosis management. J Bone Joint Surg Am 2011;93:1057–63.
[11] Schreiber JJ, Anderson PA, Hsu WK. Use of computed tomography for assessing bone mineral density. Neurosurg Focus 2014;37:E4.
[12] Lee S et al. Correlation between bone mineral density measured by dual-energy X-ray absorptiometry and hounsfield units measured by diagnostic ct in lumbar spine. J Korean Neurosurg Soc 2013;54:384–9.
[13] Pickhardt PJ et al. Opportunistic screening for osteoporosis using abdominal computed tomography scans obtained for other indications. Ann Intern Med 2013;158:588–95.
[14] Nishiyama K, Inaba F, Higashihara T, Kitatani K, Koxuka T. Radiation osteoporosis - an assessment using single energy quantitative computed tomography. Eur Radiol 1992;2:322–5.
[15] Fajardo LF. The pathology of ionizing radiation as defined by morphologic patterns. Acta Oncol 2005;44:13–22.
[16] Ratcliffe JF. The arterial anatomy of the adult human lumbar vertebral body: a microarteriographic study. J Anat 1980;131:57–79.
[17] Ratcliffe JF. Arterial changes in the human vertebral body associated with aging. The ratios of peripheral to central arteries and arterial coiling. Spine 1986;11:235–40. Phila Pa 1976.
[18] Tsai CJ et al. Osteoradionecrosis and radiation dose to the mandible in patients with oropharyngeal cancer. Int J Radiat Oncol Biol Phys 2013;85:415–20.